

Feature Based Fabrication in Layered Manufacturing

Xiaoping Qian

Debasish Dutta

Department of Mechanical Engineering,
The University of Michigan,
Ann Arbor, MI 48109
e-mail: xpqian/dutta@engin.umich.edu

To address the conflicting requirements between holding specified surface quality and decreasing build time in layered manufacturing, we present a feature-based fabrication methodology whereby the curvature effects are localized within each decomposed volume. However, staircase interaction between the boundaries of the decomposed neighboring volumes creates geometric incompatibility for deposition, which further results in undesired material properties. This paper proposes a novel concept, feature interaction volume, to eliminate the staircase interaction. Based on this concept, a feature based volume decomposition algorithm is developed. This algorithm enables each decomposed volume to be fabricated independently and compatibly. Implementation and example results are also presented. [DOI: 10.1115/1.1377282]

1 Introduction

Layered manufacturing (LM) refers to a host of fabrication technologies that build parts by depositing materials layer-by-layer. Its domain has moved beyond prototyping and now includes complex functional parts. LM makes parts without part-specific tooling or fixturing and needs fairly little human involvement.

Although the layer-wise deposition has the advantage of making complex parts easily, it also has one inherent drawback. This layer-wise deposition makes the deposition process particularly vulnerable to any local geometry variation. Typically, a point with high curvature decreases the layer thickness for the entire layer at that height. Slicing is one of the main factors that affect surface quality and build time [1]. A lot of research on slicing has been focusing on addressing this issue.

1.1 Previous Work on Slicing. Slicing determines the layer thickness and cusp-heights which in turn affect the surface quality of the part. Slicing also determines the build time since the more layers a part has, the more time it takes to fabricate the part. To overcome the conflicting requirements associated with high surface quality and low building time, adaptive slicing was proposed. This idea was to decrease slice thickness in high curvature regions to meet the cusp height requirements [2–4]. In Sabourin et al. [5] a variant was proposed whereby adaptive high-precision exterior and high-speed interior can be achieved.

However, most adaptive slicing procedures result in a time-inefficient build process. Specifically, the reduced layer thickness at one high curvature point is employed to build the entire layer. Recognizing this, new approaches have been proposed [6,7]. More recently, region-based slicing has been proposed to incorporate different surface finish requirements on one part [8]. However, these approaches do not give good criteria to decompose the part volume.

Research has also been focusing on evaluating trade-offs among build time, accuracy and surface quality [9,10]. However, compromises have to be made according to the relative importance of these conflicting objectives.

Figure 1 gives a comparison of various slicing methods. In the top-left is the example part. Figure 1(a) shows the uniform slicing. Figure 1(b) shows the adaptive slicing, in which the slant cylindrical surface at Feat2 decreases the slice thickness of the vertical surface at Feat1 and the cylindrical surface at Feat4 decreases the slice thickness of the vertical surface at Feat3. Figure 1(c) gives the slices obtained by local adaptive slicing method, in which the slicing of Feat1 is independent of Feat2. But the layer thickness of

Feat3 is still reduced due to the cylindrical surface of Feat4. Figure 1(d) shows the region-based slicing method, in which the horizontal cylindrical surface has high surface quality requirement.

In this paper, we propose a methodology to localize the curvature effects—the feature based fabrication approach. Figure 1(e) presents the feature-based slicing method proposed in this paper and all the features (Feat1, Feat2, Feat3, and Feat4) are sliced independently. Feature-based slicing enables the localization of the fabrication strategies. Furthermore, it allows the use of any particular slicing method such as adaptive slicing, local adaptive slicing, or region-based slicing, for each individual feature volume.

1.2 Staircase Interaction. Layer-wise fabrication in LM leads to the stair-case effect for slant surfaces, as shown in Fig. 2(a). (Here δ is the cusp height which is the maximum distance between the nominal part boundary and the boundary of the part produced by LM.) Depending on the intended application of the LM part one would, in general, employ excess deposition or deficient deposition [4]. Figure 2(b) and Fig. 2(c) show the two deposition situations, in which S is the desired part boundary and S' is the actual part boundary produced by LM.

For volume decomposition based fabrication (such as the feature-based fabrication proposed here), staircase interaction occurs between neighboring volumes. This staircase interaction results in geometric incompatibility. For example, in Fig. 3, a part, made of a hemisphere and a slant cylinder, is fabricated by feature-based slicing to decrease the build time [11]. If both feature A and feature B are fabricated by excess deposition, the layers in A and B would interfere with each other (Fig. 3(a)). If both feature A and feature B are fabricated by deficient deposition, a large void area is created between the neighboring layers in A and B (Fig. 3(b)). If one is fabricated by excess deposition and the other by deficient deposition, the interaction typically results in both interference and void since the layer thickness of A and B do not match (Fig. 3(c)). The layers of A and B become compatible when the build direction of A is the same as B and the layer thickness of A and B are exactly the same (Fig. 3(d)). However, this compatibility is achieved by sacrificing the fabrication independence between neighboring volumes. The staircase interaction poses more problems for multiple direction deposition. For example, with same layer thickness for neighboring volumes, one by deficient fabrication and one by excess fabrication, the staircase interaction results in both interference and void areas, as shown in Fig. 4 (Z1 and Z2 indicate different build directions for hemisphere and slant cylinder).

This geometric incompatibility, i.e. the presence of interference and void, leads to undesired material properties, such as material

Contributed by the General and Machine Element Design Committee for publication in the JOURNAL OF MECHANICAL DESIGN. Manuscript received Nov. 1999. Associate Editor: J. M. Vance.

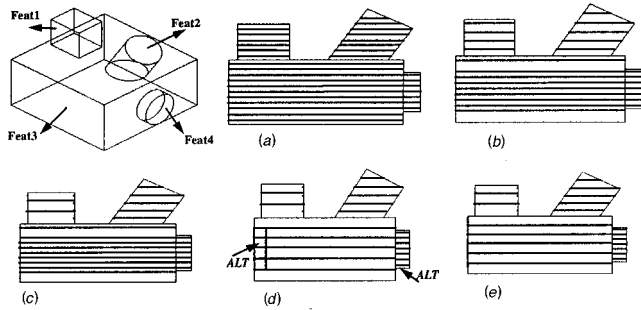


Fig. 1 Comparison of various slicing methods: (a) uniform slicing; (b) adaptive slicing; (c) local adaptive slicing; (d) region-based slicing; (e) feature-based slicing

distortion, weakened bonding strength, etc. (See Section 4.2). In this paper, we propose feature interaction volume, which will be explained fully in the following sections, to eliminate the staircase interaction for feature-based fabrication.

The remainder of this paper is organized as follows. Section 2 reviews feature interaction and introduces feature interaction loop

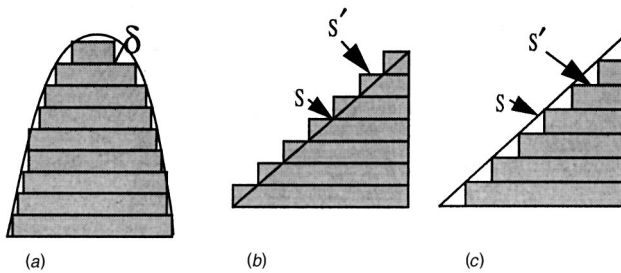


Fig. 2 Staircase effect and different deposition situations: (a) staircase effect; (b) excess deposition; (c) deficient deposition

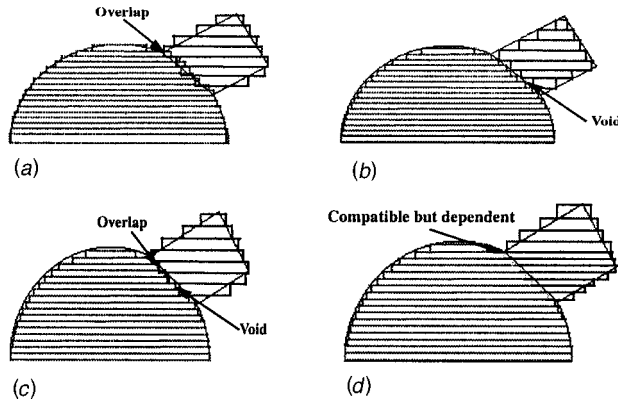


Fig. 3 Staircase interaction: (a) excess+excess; (b) deficient+deficient; (c) deficient+excess; (d) deficient+excess

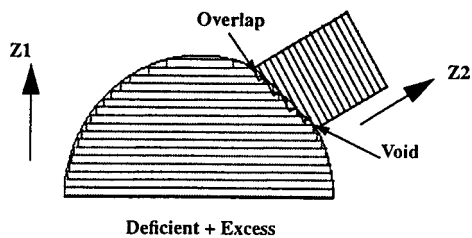


Fig. 4 Staircase interaction for features with different build directions

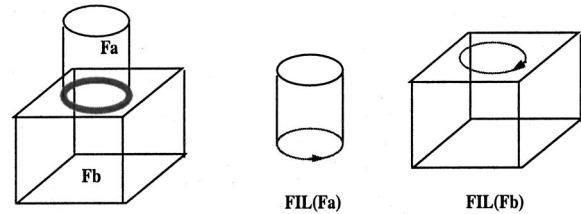


Fig. 5 FIL and its direction

(FIL) and feature interaction surface (FIS) to characterize the feature interaction for LM. Section 3 presents the concept of feature interaction volume, the staircase-interaction free strategy and the algorithm for the volume decomposition. Section 4 describes the implementation and experimental results of the staircase interaction and build time saving by feature-based fabrication. Section 5 analyzes the build time saving by the curvature localized fabrication. Finally the paper is summarized in Section 6.

2 Feature Interaction Characterization for LM

Features have been widely and successfully used in design, process planning and manufacturing processes. For a review of feature technology, refer to [12]. In the context of layered manufacturing, features have been proposed to facilitate the design and fabrication of the heterogeneous objects [13].

To decompose part volume according to features, feature interaction processing is a critical issue. Although feature interaction has been addressed in the NC machining domain [14], it has not been explored in LM domain. This section reviews how features interact with each other. We propose FIL and FIS to be used to describe feature interactions for different situations in the LM domain.

Feature interaction refers to the situations where two or more features intersect. Two features F_i and F_j ($i \neq j$) are interacting when $F_i \cap F_j \neq \emptyset$. Note, the intersection operation is a non-regularized operation.

Feature adjacency refers to situations where features share the same topological entities, such as edge(s) or face(s), in the part volume. We refer to such features as adjacent features.

To systematically handle feature interactions, we classify them into the following two categories: (1) interaction between additive features or between subtractive features; (2) interaction between an additive feature and a subtractive feature. Interaction resulting from the surface features, such as fillet and chamfer, can be considered as a special case of interaction between additive feature and subtractive feature. Note, support volume in LM is considered as a subtractive feature.

For the first category of feature interaction, a *feature interaction loop* is identified to describe the interaction. For the second category of feature interactions, *feature interaction surface* is identified. Both are described in the next section.

2.1 Interaction between Additive Features or Between Subtractive Features

2.1.1 Feature Interaction Loop. When one feature intersects with another, a feature interaction loop (FIL) is formed. FIL carries direction indicating which side contains the feature, according to the anti-clock-wise convention. In Fig. 5, F_a intersects with F_b . Two FILs are identified, $FIL(F_a)$ and $FIL(F_b)$, each carrying a direction as shown in Fig. 5. This direction can be easily obtained by copying the direction of each component edge within the FIL. That is, the directions of the edges in the adjacent faces of the FIL form the direction of FIL.

Therefore, more formally, when adjacent features intersect, we refer to the closed (loop) curve of intersection as the FIL.

Note, FIL can be formed by the intersections of two or more than two features (Figs. 6(a), and 6(b)), and we refer to them as simple FIL and compound FIL respectively.

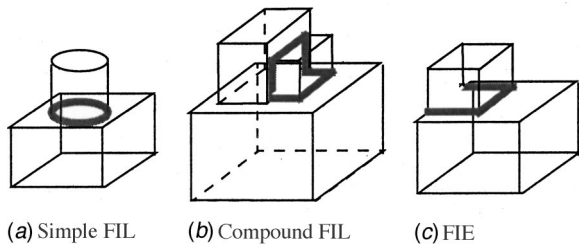


Fig. 6 Feature interaction edge and feature interaction loop: (a) simple FIL; (b) compound FIL; (c) FIE

In some interaction situations, FIL may not appear as a closed loop. In such cases, only a feature interaction edge (FIE) exists in the part model (Fig. 6(c)). We obtain FIL by processing the FIE. This step converts FIEs into FIL by intersecting the adjacent features of the FIEs. Figure 7 lists the steps in FIE processing. Suppose FIE has adjacent features F_a and F_b . We intersect F_a and F_b and get the volume V_{ab} (non-regularized intersection). From the volume V_{ab} , we form the FIL and map the FIL into the part model.

After the FIE processing, all interactions between additive features or between subtractive features, can be represented by FILs.

2.1.2 FIL Cluster. FIL cluster is a collection of FILs that are adjacent to each other. That is, within an FIL cluster, all the FILs are topologically connected and each edge is traversed twice along opposite directions. For example, in Fig. 8, F_a and F_b intersect. The FIL cluster includes $FIL(F_a)$ and $FIL(F_b)$, which carry opposite directions.

For compound FILs, an FIL cluster can consist of more than two FILs. An example is shown in Fig. 9, in which $FIL(F_a)$, $FIL(F_b)$ and $FIL(F_c)$ together form an FIL cluster. Within this FIL cluster, each component, FIE, is traversed twice in opposite directions.

2.2 Interaction Between Additive Feature and Subtractive Feature. Feature Interaction Surface (FIS) is a surface that separates a feature from its neighboring volumes in the part. One example is shown in Fig. 10(a). Two surfaces of the hole, one bottom surface and one side cylindrical surface, separate the hole

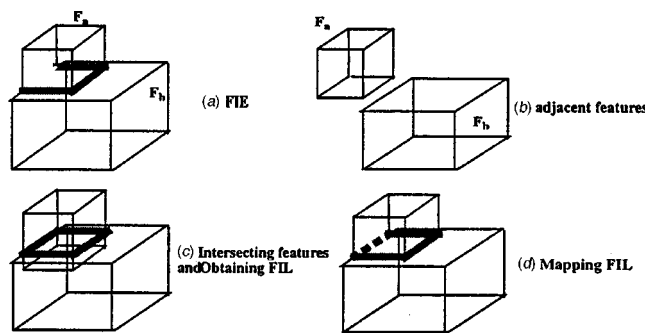


Fig. 7 FIE processing

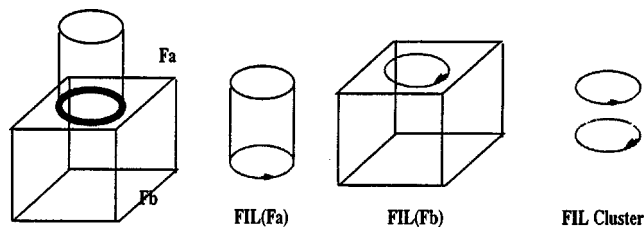


Fig. 8 Simple FIL and FIL cluster

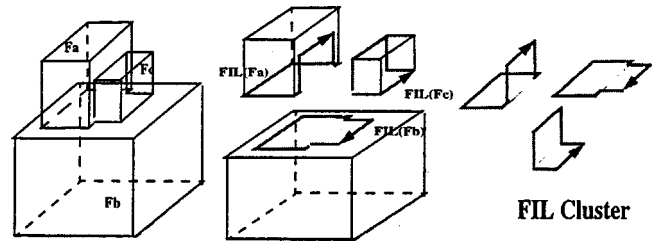


Fig. 9 Compound FIL and FIL cluster

from the hemisphere and are referred to as FISs. When an additive feature and a subtractive feature interact with each other, the surfaces of the subtractive feature that remain in the resultant volume separate the additive feature volume from subtractive volume. We refer to these as FISs. Another way to consider FIS is to think of additive feature and subtractive feature as volumes made of different materials. The FIS separates one material from the other. The surface normal indicates which side contains the feature.

Surface features, such as fillet, blend, chamfer, etc. are often used in commercial feature modeling packages. To localize the fabrication, feature interactions due to surface features can also be identified and characterized by the feature interaction surface. An example is shown in Fig. 10(b). The curved surface is a surface feature in the design and is also an FIS that separates the part from the void area.

To summarize, feature interactions can be characterized either by FIL (Cluster) or by FIS regardless of the interaction type. Both FIL and FIS carry the directions indicating which side has the feature.

3 Staircase Interaction Free Volume Decomposition Algorithm for LM

3.1 Staircase Interaction Free Strategy. To eliminate the staircase interaction for each feature interaction, we propose the following two concepts:

Feature interaction volume (FIV) is a transition volume formed to eliminate the staircase interaction between adjacent feature volumes.

Refined feature volume (RFV) is a feature volume devoid of all of its feature interaction volumes.

For example, in Fig. 11(a), features are to be fabricated along vertical direction Z. An FIV is formed with the vertical and horizontal parting surface. This FIV eliminates the staircase interaction, and the adjacent RFVs can be fabricated independently and compatibly. In Fig. 11(b) an FIV is generated for the features with different build directions.

Still the separating surfaces of RFVs is either perpendicular or parallel to the build directions of the features. So there is no staircase interaction.

Before we present the staircase interaction free strategy, we present the following Lemma.

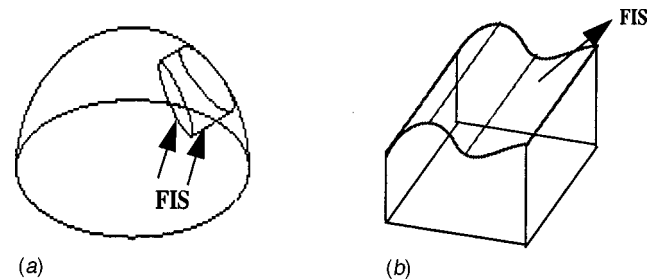


Fig. 10 Subtractive feature, surface feature and feature interaction surface: (a) subtractive feature; (b) surface feature

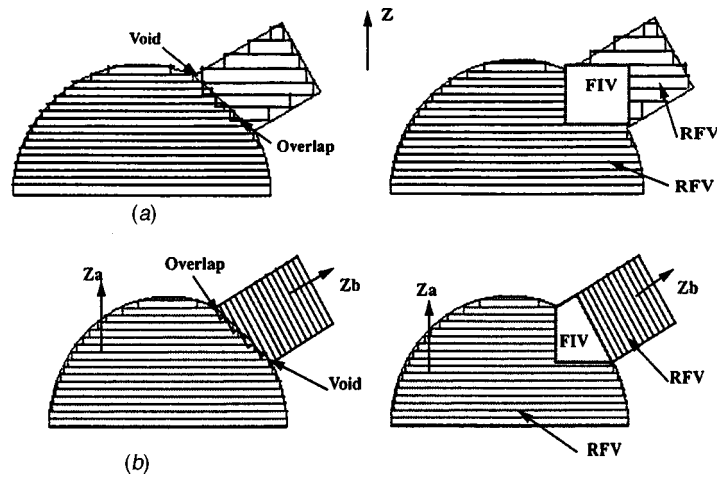


Fig. 11 FIV eliminating staircase interaction: (a) features with same build direction: (b) features with different build directions

Lemma: If the surfaces, $\{S\}$, separating RFV from the neighboring volumes satisfy the following constraint: $S \parallel Z$, or $S \perp Z$, there is no staircase interaction between the RFV and the neighboring volumes.

Based on the above Lemma, we can have the following staircase-interaction free strategy. At each feature interaction area, a transition volume, FIV, is created so that the parting surfaces that separate RFV from the neighboring volumes are either perpendicular or parallel to the build direction of the features. So there is no staircase effect on RFVs and consequently there is no staircase interaction between any neighboring volumes.

For any FIL or FIS, the projecting profile and the projected surface along the build direction is parallel and perpendicular respectively to the build direction. Therefore, a projecting volume of FIL or FIS can be used to decompose the feature volumes. By forming FIV based on the projection volume, staircase effect on RFV is eliminated and the staircase interaction between the RFV and FIV also disappears. So the volumes can be fabricated independently and compatibly.

Therefore, a staircase-interaction free strategy involves a volume decomposition problem as follows:

Given the feature set $F = \{F_1, F_2, \dots, F_n\}$, the associated build directions $Z = \{Z_1, Z_2, \dots, Z_n\}$ and the part volume PV, determine a set of decomposed volumes $V = \{V_i | V_i \in \{RFV, FIV\}\}$ such that

- 1 $PV = \cup_i V_i$
- 2 Each V_i can be sliced independently.
- 3 Each V_i can be fabricated compatibly with the neighboring volumes.

3.2 Staircase Interaction Free Volume Decomposition Algorithm. We now describe the staircase interaction free decomposition algorithm. It first collects the FILs and FISs for all the feature interactions. It then processes FIL and FISs separately and generates an FIV for each feature interaction. Finally the FIVs are subtracted from the part volume and the RFVs are generated.

Figure 12 presents an example of volume decomposition for two intersecting cylinders. The processing of the feature interaction includes the following steps: (1) identifying the feature interaction surface and/or feature interaction loop; (2) obtaining the heights of the top point (ZT) and bottom point (ZB) along the build direction at each feature interaction surface and/or feature interaction loop; projecting the FIL/FIS onto a horizontal plane and get the projection P; (3) extruding the projection P from ZB to ZT; (4) intersecting the extruded volume T with the part volume to get the feature interaction volume; (5) generating the refined feature volume.

We describe the general algorithm in detail as follows.

STEP 1: Collect all the FILs and FISs.

For each feature F_i , depending on the feature interaction type, we obtain the FILs or FISs. If the interaction is between the same type of features, FIL is obtained. Otherwise, FIS is obtained. Note, FIE processing is used to convert the non-closed loop into FIL as described in Section 2.

STEP 2: FIL processing to generate FIV

For each interaction between the same type of features, i.e., feature interactions between additive features or between subtractive features, an FIV is formed. The detailed process contains two steps, FIL cluster forming and Converting FIL cluster into FIV.

STEP 2.1 FIL cluster forming

Each feature interaction can be characterized by an FIL cluster. The algorithm is shown in Fig. 13.

STEP 2.2 Converting FIL cluster into FIV

From each FIL cluster we form an FIV. For each FIL_i within an FIL cluster, we assume the build direction is Z_i . The formation of an FIV from an FIL cluster involves three procedures. Each is described, in sequence, below.

STEP 2.2.1 Generate an un-bounded projection volume for each FIL_i

For each FIL_i

- a.) Get the top point (ZT) and bottom point (ZB) of FIL_i along Z_i (Fig. 14(a)).
- b.) Project FIL_i into the bottom plane with normal Z_i and passing through ZB, to get the FIL' . Since FIL_i carries direction, FIL' also carries a direction, noted as $dir(FIL')$, which is either the same as Z_i or the opposite of Z_i (Fig. 14(b)).
- c.) Select any point Va in the FIL and the corresponding projection point Vb in FIL' . If direction $(Va-Vb)$ is the same as $dir(FIL')$ (Fig. 14(c)), form a projection volume FIV (Fig.

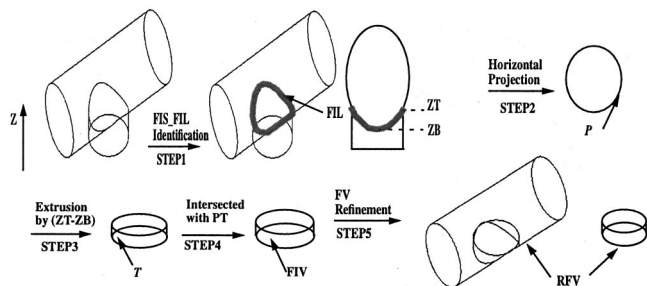


Fig. 12 Processing of feature interaction

Algorithm 1: FIL Cluster Forming Algorithm

Input: FIL set = { $FIL_1, FIL_2, \dots, FIL_m$ }

Output: FIL clusters

Algorithm:

Set each FIL_i as a separate FIL cluster (i);

For ($i=1; i<m; i++$)

 For ($j=i+1; j<=m; j++$)

 {
 Intersect FIL Cluster (i) and FIL Cluster (j);
 If FIL Cluster (i) and FIL Cluster (j) share at least one common edge,
 merge FIL Cluster (i) and FIL Cluster (j) into one FIL cluster;
 Set the new merged FIL cluster as FIL Cluster (j);
 Set the FIL Cluster (i) as NULL;
 }

return the non-null FIL cluster.

Fig. 13 FIL cluster forming algorithm

14(d1)). Otherwise, project FIL along $-Z_i$ into the plane that has the normal $-Z_i$ and passes through ZT (Figure 14(c2)) and form a projection volume FIV (Fig. 14(d2)). Note, this FIV is not a bounded volume since one surface bounded by FIL_i is undefined.

STEP 2.2.2: Merge unbounded projection volume

All the volumes generated from the FIL s are merged to form a closed solid FI_EV . That is, $FI_EV = \cup_i FIV_i$.

An example of the unbounded volume merging is shown in Fig. 15. In Fig. 15(a) the FI_EV is formed with the same build direction. Figure 15(b) shows the volume merging for the features with different build directions.

Note, $FIV(Fa)$ and $FIV(Fb)$ are unbounded volumes. The union of the FIV s forming from an FIL cluster forms a bounded solid.

STEP 2.2.3: Form FIV

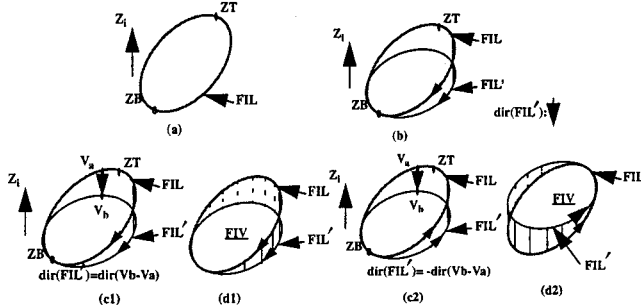


Fig. 14 FIL projection and volume forming

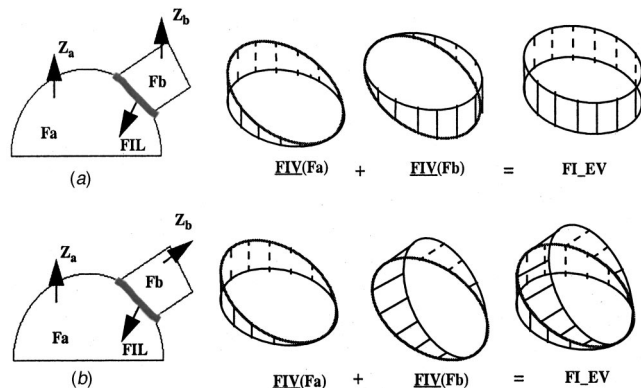


Fig. 15 Non-closed volume merging: (a) same build direction; (b) different build direction

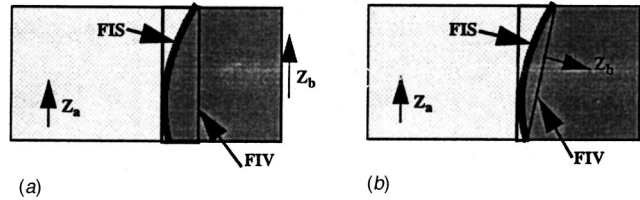


Fig. 16 FIS enabling volume decomposition: (a) same build direction ($Z_a=Z_b$); (b) $Z_a \neq Z_b$

Due to the fact that projected volumes may penetrate the feature boundary, an intersection of the merged volume with the interaction features is performed to get the FIV . That is,

$$FIV = FI_EV \cap \cup_i F_i = \cup_i FIV_i \cap \cup_i F_i$$

STEP 3: FIS Processing

Each FIS has two adjacent features $F1, F2$ and two corresponding build directions $Z1, Z2$. The procedures to form an FIV for each FIS is similar to the FIV forming procedures for the FIL clusters. The three procedures are described below.

STEP 3.1: Projection volume generation for each side of FIS

An FIV_i can be formed for each feature by projecting FIS along Z_i from the bottom point to top point. Note, FIV formed from FIS is a bounded solid. This is the difference between the FIV generated from FIS and the FIV from FIL .

STEP 3.2: Projection volume Merging

$$FI_EV = \cup_i FIV_i$$

STEP 3.3: FIV Creation

$$FIV = FI_EV \cap \cup_i F_i = \cup_i FIV_i \cap \cup_i F_i$$

In Fig. 16 are two FIV formed for different situations. In Fig. 16(a), the two adjacent features of FIS have the same build directions ($Z_a=Z_b$), while in Fig. 16(b), the build directions are different ($Z_a \neq Z_b$). In both cases, FIV s are formed by the projection volumes that project FIS along the build directions of the adjacent features.

STEP 4: FIV Union

Since the FIV s generated at different feature interaction locations may interact with each other, and may lead to staircase interaction again, the FIV s are combined. That is, the FIV set is a union of all the FIV s.

$$\{FIV\} = \cup_i FIV_i$$

STEP 5: Generating RFV

The final RFV s are generated by subtracting the FIV set from the part volume. That is,

$$\{RFV\} = PV - \{FIV\}$$

The five step procedure is summarized by the algorithm shown in Fig. 17.

3.3 Discussion. The FIV and its processing algorithm have many desirable properties. Due to space restrictions, we only highlight a few of them here. For a lengthy discussion, refer to [15]

- (Local Behavior) Changes in one feature's build direction only affects that feature's RFV .
- (Staircase-interaction free) FIV eliminates the staircase interaction between the decomposed volumes, i.e. RFV s and FIV . It also completely eliminates the staircase effect of the parting surfaces when the decomposed volumes are fabricated in one direction.

Algorithm: Staircase interaction free volume decomposition for LM

STEP 1: collecting FILs and FISs

Obtain FIL or FIS for each interaction

STEP 2: FIL Processing

Cluster FILs into a set of FIL clusters (*FIL cluster forming algorithm*)

For each FIL cluster

Generating projection volume \underline{FIV}_i for each FIL_i

Merge projection volume $\bigcup_i \underline{FIV}_i$

Forming FIV: $FIV = \bigcup_i \underline{FIV}_i \cap \bigcup_i F_i$

STEP 3: FIS Processing

For each FIS

Generating projection volume \underline{FIV}_i for each FIS_i

Merge projection volume $\bigcup_i \underline{FIV}_i$

Forming FIV: $FIV = \bigcup_i \underline{FIV}_i \cap \bigcup_i F_i$

STEP 4: FIV Union

$\{FIV\} = \bigcup_i FIV_i$

STEP 5: Generating RFVs

$\{RFV\} = PV - \{FIV\}$

Fig. 17 Staircase interaction free volume decomposition algorithm

- (Independence) The slicing of each decomposed volume, RFV or FIV, is independent from the slicing of any neighboring volumes.
- (Uniqueness) The feature interaction processing algorithm creates unique FIV(s) regardless of the processing order of feature interactions.

4. Implementation

4.1 Implementation of Feature-Based Fabrication. The volume decomposition algorithm has been implemented on a SUN workstation using C++ and the ACIS geometric modeling kernel. The input is a feature based CAD model and the output is the decomposed RFVs and FIVs. An in-house software Adaptive Slicing Module [4] is used to slice each of the decomposed volumes. The parts are fabricated by Stratasys FDM 1650 machine.

Since our current LM machine cannot deposit materials in multiple directions, all the features are assumed to have the same build direction. However, the feature interaction processing algorithm has been developed for features with multiple build directions.

4.2 Experimentation of Staircase Interaction Effects. Experiments were conducted to compare the decomposed volume interaction with and without the feature interaction processing.

For the part shown in Fig. 3, the microscopic pictures of different interaction scenarios are shown in Fig. 18. Note, only half of the part is fabricated to observe the interface. Figure 18(a) shows the layer distortion created during the excess-excess deposition scenario. Figure 18(b) shows the voids created during the deficient-deficient deposition process. Figures 18(c) and (d) reveal that both the distortion and voids exist in the excess-deficient deposition process. Figure 18(e) shows the layer interface of vertical parting surface due to the FIV.

To quantify the dimensional accuracy loss and material strength deterioration caused by the staircase interaction, further experiments were conducted. A set of $0.5\text{ in} \times 0.2\text{ in} \times 4\text{ in}$ bars were fabricated with different deposition strategies for the volumes separated by the slant surface P (Fig. 19). Refer to [15] for the details of the experiments. The results are shown in Table 1. Note,

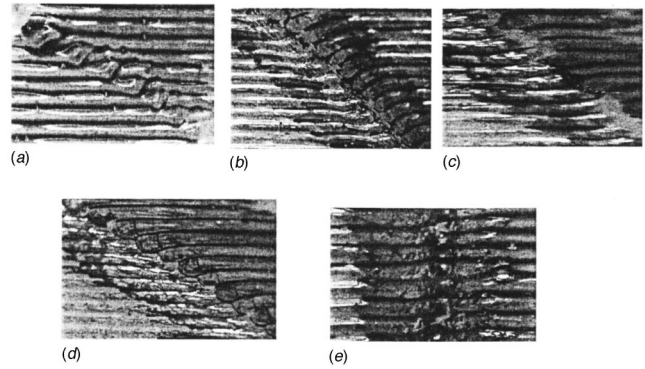


Fig. 18 Staircase interaction with/without vertical parting surface: (a) overlap in excess-excess deposition; (b) void in deficient-deficient deposition; (c) void in excess-deficient deposition (d) overlap in excess-deficient deposition; (e) compatible deposition

no test on excess-deficient deposition was conducted since the interaction under excess-deficient deposition will vary from surface to surface, depending on the layer thickness of the neighboring volumes.

The dimensional accuracy experiments show that compatible deposition results in parts with tolerance an order of magnitude lower than excess-excess deposition. Note, here the dimensional accuracy refers to the flatness. The parts made by deficient-deficient deposition and compatible deposition due to the FIV exhibit the same tolerance, 0.006 in , as the parts fabricated by the uniform slicing method. However, for deficient-deficient deposition, a strip of void was visible even by the naked eye at some angle (observed in the experiment, when $\alpha=45\text{ deg}$) (Fig. 20(a)). For excess-excess deposition, this stack of distortion and overlap leads to poor geometric accuracy, particularly in the Z direction and the front surface. A strip of protruded area appeared in the front/back surfaces and the top surface. Figure 20(b) shows a front view of the protruded area. Along the Z-direction, depending on the slant angle α , a strip protrudes about $0.02\sim 0.05\text{ in}$ high and $0.04\sim 0.06\text{ in}$ wide. On the front surface, the distortion was observed, ranging from 0.02 to 0.03 in , while the width is about $0.01\sim 0.06\text{ in}$.

The tensile strength tests show that parts made by excess-excess deposition and by compatible depositing exhibit considerably higher strength than those parts by deficient-deficient deposition. Due to the loose bonding in the deficient-deficient deposition, the tensile strength is below 230N. The broken surface strictly follows the interface that separates the neighboring volumes (Fig. 20(a)). This is due to a very loose bonding at the interface area. For the parts made in excess-excess deposition, when $\alpha>30\text{ deg}$, the parts tend to fail because of the necking; when $\alpha<30\text{ deg}$, the failures due to the necking and failures at the weakened bonding between the contour path and raster path (Fig. 20(b)) were both observed. For the compatible deposition by FIV,

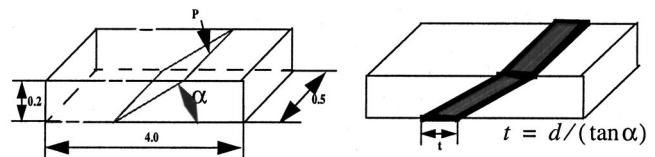


Fig. 19 Staircase interaction testing part: (a) test part; (b) a strip of overlap/void area in excess-excess/deficient-deficient deposition

Table 1 Dimensional accuracy and strength comparison of different layer interactions

Item	Deficient-Deficient	Excess-Excess	Compatible deposition
Dimensional Accuracy	0.006in void is visible sometimes	0.05in protuded area of 0.02-0.05in high and 0.04-0.06in wide	0.006in
Tensile Strength	0-230N	600-770N	500-600N ..

the parts tend to fail at the weakened bonding between the contour path and the raster path, although the failure caused by necking were also observed.

The dimensional and strength test experiments indicate that

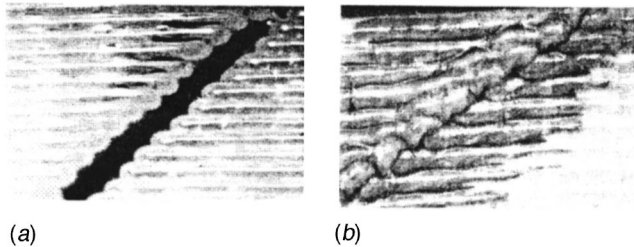


Fig. 20 Front views of testing part with visible dimensional defects: (a) a strip of void in deficient-deficient deposition; (b) a strip of protruded area in excess-excess deposition

Table 2 Time comparison of different methods

Method	Time (hr)
Adaptive Slicing	7.3
Local Adaptive Slicing	7.1
Feature-based Slicing	5.6

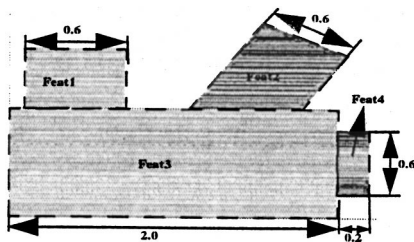


Fig. 21 Example 1 (FIV=nil)

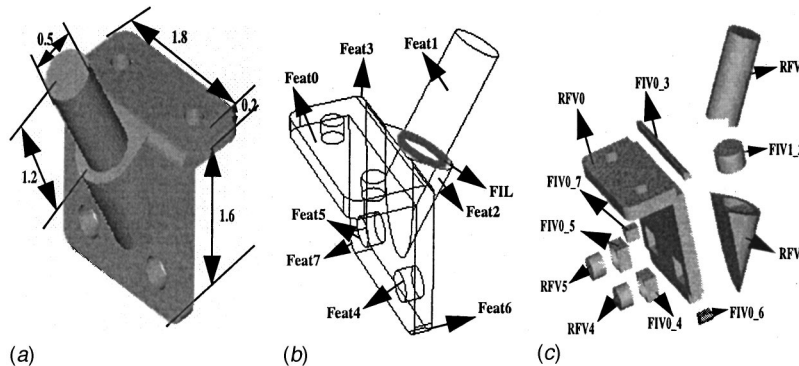


Fig. 22 Example 2 (with FIVs): (a) example part 2; (b) features in the part; (c) exploded view of decomposed RFVs and FIVs

compatible deposition by the vertical parting surface introduced by FIV gives overall better dimensional accuracy, surface quality, and higher strength.

4.3 Build Time Saving by Feature-Based Fabrication. We now consider build time savings due to feature-based fabrication and discuss results from the experiments.

Example 1 (FIV=nil) In this example, FIV is null. Different slicing methods were used to build the sample part of Fig. 1, and the build time comparison is given in Table 2. Note, the build time includes the time taken to build the support under *Feat4*. Since feature-based slicing can also incorporate region-based slicing for each individual volume, we do not include region-based slicing in Table 2. Figure 21 shows the slices in each individual feature by the feature-based slicing method. In this example, the cusp height is 0.005 in, minimum layer thickness is 0.002 in and maximum layer thickness is 0.015 in. The boundary box of the part is 2.2 in × 2 in × 1.8 in. The key dimensions of the part are shown in Fig. 21. As Table 2 shows, nearly one third of the build time is saved by using feature-based slicing instead of adaptive slicing or local adaptive slicing. The slicing was done independently for four feature volumes and slices were finally merged together.

Example 2 (with FIVs). In Example 2 (Fig. 22), the sample part (downloaded from NIST repository with a scale 0.02 [16]) was also sliced by the adaptive slicing, local adaptive slicing and feature-based slicing method. For this part, there are FIVs generated by the volume decomposition algorithm. Figure 22(b) shows a list of those features in the example part that have FIVs. An FIV is generated for each feature interaction and the feature volumes are refined. For instance, the bold dark line in Fig. 22(b) is an FIL between *Feat1* and *Feat2*. *FIV1_2* is then created for the feature interaction between *Feat1* and *Feat2* as shown in Fig. 22(c). After the FIV is generated, the features are refined and *RFV1* and *RFV2* are obtained respectively from *Feat1* and *Feat2*.

After all the volumes are obtained, adaptive slicing is done separately for each volume. In this example, the cusp height for the part is 0.005 in. The minimum layer thickness is 0.002 in and the maximum layer thickness is 0.015 in. The boundary box of

Table 3 Time comparison for various methods

Methods	Time(hr)
Adaptive Slicing	3.8
Local Adaptive Slicing	3.8
Feature-based Slicing	3

this part is 2.8 in × 1.8 in × 2.7 in. The key dimensions of the part are shown in the Fig. 22(a). The time comparison is shown in Table 3. Note, the build time for the underneath support structure is approximately 1.6 hours and is not included in the time shown in Table 3. Feature-based slicing yields a savings of 27 percent build time when compared to adaptive slicing method and local adaptive slicing method.

5 Build Time Analysis for Localized Fabrication

As described in Section 1, decreasing build time by localizing curvature effects has been explored by some researchers. Localized fabrication saves build time by decreasing the number of layers over relatively flat areas. However, the total number of layers is still larger than the layers by uniform slicing. Due to the extra time for switching layers during the fabrication, the localized fabrication may not necessarily lead to build time saving. None of the previous approaches quantitatively analyzes the condition that will guarantee the build time saving by localized fabrication. In region-based slicing, it has been pointed out that a threshold size exists for the method to save build time but with no quantification of the size [8].

To quantitatively analyze the condition of the build time saving, we represent the approximate build time for uniform deposition and localized deposition by Eq. (1) and Eq. (2) respectively. The variables (Table 4) in these equations are as follows:

$$T_u = \frac{1}{wv} \cdot \sum_{i=1}^{N^u} A_i + N^u \cdot T_i \tag{1}$$

$$T_l = \frac{1}{wv} \sum_{j=1}^{N_f} \sum_{i=1}^{N_j^l} A_{j_i} + \sum_{j=1}^{N_f} (N_j^l \cdot T_i) \tag{2}$$

In the above equations, $\sum_{i=1}^{N^u} A_i > \sum_{j=1}^{N_f} \sum_{i=1}^{N_j^l} A_{j_i}$ since uniform deposition typically has more layers than localized deposition does over the small vertical curvature areas. Also $N^u < \sum_{j=1}^{N_f} N_j^l$ since the localized deposition results in more number of layers than uniform deposition. Therefore, it is not certain that localized fabrication method will lead to build time reduction.

To further investigate the situations where localized fabrication always reduces build time, we illustrate the comparison of two fabrication methods. In Fig. 23, we assume the number of layers

Table 4 Notations

T_u	build time for uniform deposition	T_l	build time for localized deposition
T_i	idle time between each layer	w	deposition road width
v	nozzle speed	A_i	area of the i -th layer in uniform deposition
A_{j_i}	i -th layer in j -th feature	N_u	number of layers for uniform deposition
N_f	number of decomposed volumes	N_j^l	l layers in the j -th features

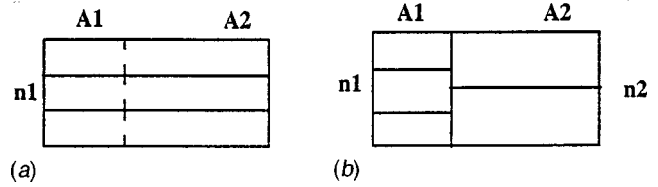


Fig. 23 Time comparison of two fabrication methods: (a) uniform deposition; (b) localized deposition

n_1 at area A1 by localized deposition is no less than the number of layers n_2 at area A2, i.e. $n_1 \geq n_2$. The build time for these two approaches are described in Eq. (3) and Eq. (4).

$$T_u = n_1 \left(\frac{A_1}{wv} + \frac{A_2}{wv} \right) + n_1 T_i \tag{3}$$

$$T_l = n_1 \cdot \frac{A_1}{wv} + n_2 \cdot \frac{A_2}{wv} + (n_1 + n_2) \cdot T_i \tag{4}$$

The difference in build time is now given by

$$T_u - T_l = (n_1 - n_2) \cdot \frac{A_2}{wv} - n_2 \cdot T_i \tag{5}$$

The above equation can be easily extended to situations where there are N_f decomposed volume ($N_f \geq 2$).

$$T_u - T_l = \sum_{j=2}^f \left(\underbrace{(n_1 - n_j) \cdot \frac{A_j}{wv}}_{T_1} - \underbrace{n_j \cdot T_i}_{T_2} \right) \tag{6}$$

In summary, the build time difference by localized slicing method and uniform slicing method consists of two parts, deposition time difference T1 and layer switching time difference T2. T1 is the time saving by localized deposition due to the saving of layers in some relatively flat features. T2 is the time increase due to the increase of number of total layers. So only when a feature size is larger than certain threshold, the feature-based slicing will lead to build time savings.

To further illustrate this, Eq. (5) can be re-written as Eq. (7)

$$T_u - T_l = n_2 \cdot \frac{A_2}{wv} - n_1 \cdot \left(\frac{A_2}{wv} + T_i \right) \tag{7}$$

From the (Eq. (7)), we observe the following:

Observation 1. If $A_2/wv > 10 \cdot T_i$, $T_u - T_l \approx n_2 \cdot A_2/wv - n_1 \cdot A_2/wv$ and the idle time effect is negligible. We can have

$$T_u - T_l = (n_2 - n_1) \cdot \frac{A_2}{wv} \tag{8}$$

Since $n_2 \geq n_1$, it is clear that localized fabrication always saves build time.

From Eq. (8), it can be inferred that the build time saving is mainly dependent on the area of A2 (lower curvature area) and the difference in the number of layers in A2. Also the build time

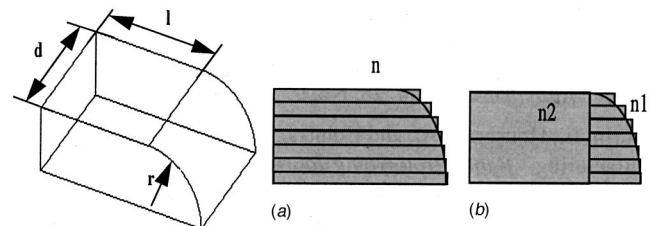


Fig. 24 Benchmark part for time comparison of two fabrication methods: (a) uniform fabrication; (b) localized fabrication

Table 5 Time comparison of feature size's effect over build time

Part No	d (in)	l (in)	r (in)	A (in ²)	Build Time by Uniform (n=55)	Build Time by Localized I (n1=55, n2=34)	Build Time by Localized II (n1=55, n2=50)
1	1	1	0.5	1	102 min	79 min	98 min
2	1	0.5	0.5	0.5	68 min	59 min	68 min
3	1	0.3	0.5	0.3	54 min	49 min	56 min

saving is independent of high curvature area A_1 , which implies that the size of high curvature area has no effect on build time saving.

Observation 2. If $A_2/wv < 10 \cdot T_i$, localized fabrication method reduces build time only when n_2 is much larger than n_1 . This happens when high precision parts are desired so that any small curvature difference leads to significant layer number difference, i.e. $n_2 \gg n_1$.

Hence we propose the following rule of thumb.

Localized fabrication saves build time if $A_i/wv > 10 \cdot T_i$, where A_i is the area of lower curvature area (i.e., relatively less number of slices exists in these areas).

Experiment (Verification of the rule of thumb)

To verify the rule of thumb, an experiment was devised on Stratasys FDM 1650 machine. In FDM machine, by observation, we have the following parameters: $w = 0.02$ in, $v = 0.7$ in/sec, $T_i = 4.0$ sec (Ti-including idle time between layers, along with the Z movement and nozzle starting and stopping time- determined experimentally), the critical area $A_i = 10 \cdot T_i \cdot wv = 0.56$ in².

Experiments were done for the benchmark part shown in Fig. 24 by varying the size of the block feature. The results are shown in Table 5.

From Table 4, it is confirmed that (1) when the area of relatively flat region is larger than the threshold size (0.56 in²), localized fabrication always leads to build time saving regardless of the difference in the number of layers; (2) when the area is smaller than the threshold size, only significant difference in the number of layers, ($n_1 - n_2$), can lead to build time saving.

6 Summary

This paper presents a feature-based fabrication methodology in LM domain to resolve the dilemma between improving the surface quality and decreasing the build time. A novel concept, feature interaction volume, is proposed to eliminate the staircase interaction between the neighboring volumes. Based on this, the staircase-interaction free volume decomposition algorithm is developed to enable the compatible and independent fabrication of each decomposed volume.

Experimental results and quantitative analysis demonstrate that significant build time can be saved by using feature-based fabrication method. Feature-based fabrication is an effective way to localize curvature effects. FIV successfully eliminates the staircase interaction which leads to better surface quality and material strength than otherwise.

Although the study was conducted only on a Stratasys FDM machine, we believe that the feature-based fabrication method can

be applied to LM processes such as Stereolithography (SLA), Selective Laser Sintering (SLS), and LOM, etc. which can fabricate parts with varying layer thickness in different regions.

Acknowledgments

We gratefully acknowledge the financial support from NSF (grant MIP-9714751) and ONR (grant N00014-97-1-0245).

References

- [1] Tumer, I., Thompson, D., Wood, K., and Crawford, R., 1998, "Characterization of Surface Fault Patterns with Application to a Layered Manufacturing Process," *J. Manuf. Syst.*, **17**, No. 1, pp. 23–36.
- [2] Suh, Y. S., and Wozny, M. J., 1994, "Adaptive Slicing of Solid Freeform Fabrication Processes," *Proceedings of Solid Freeform Fabrication Symposium*, The University of Texas at Austin, August 8–10, pp. 404–411.
- [3] Dolenc, A., and Makela, I., 1994, "Slicing Procedure for Layered Manufacturing Techniques," *Computer-Aided Design*, **26**, No. 2, pp. 119–126.
- [4] Kulkarni, P., and Dutta, D., 1996, "An Accurate Slicing Procedure for Layered Manufacturing," *Computer-Aided Design*, **28**, No. 9, pp. 683–697.
- [5] Sabourin, E., Houser, S. A., and Bohn, J. H., 1997, "Accurate Exterior, Fast Interior Layered Manufacturing," *Rapid Prototyping Journal*, **3**, No. 2, pp. 44–52. Thesis: <http://www.cadlab.vt.edu/bohn/projects/sabourin/>
- [6] Krause, F. L., Ulbrich, A., Ciesla, M., Klocke, F., and Wirtz, H., 1997, "Improving Rapid Prototyping Processing Speeds by Adaptive Slicing," *Proceedings of Sixth European Conference on Rapid Prototyping and Manufacturing*, Dickens, P. M., ed., Nottingham, UK, July 1–3, pp. 31–36.
- [7] Tyberg, J., and Bohn, J. H., 1998, "Local Adaptive Slicing," *Rapid Prototyping Journal*, **4**, No. 3, pp. 118–127. Thesis: <http://www.cadlab.vt.edu/bohn/projects/tyberg/>
- [8] Mani, K., Kulkarni, P., and Dutta, D., 1999, "Region-based Adaptive Slicing," *Computer-Aided Design*, **31**, pp. 317–333.
- [9] Onu, S. O., and Hon, K. K. B., 1998, "Optimizing Build Parameters for Improved Surface Finish in Stereolithography," *Int. J. Mach. Tools Manuf.*, **38**, No. 4, pp. 329–392.
- [10] West, A. P., and Rosen, D. W., 1999, "A Process Planning Method for Improving the Build Performance in Stereolithography," 1999 ASME Design Engineering Technical Conferences, Sep 12–15, Las Vegas, Nevada.
- [11] Qian, X., and Dutta, D., 1999, "Feature-based Slicing for Layered Manufacturing," 1999 ASME Design Engineering Technical Conferences, Sep 12–15, Las Vegas, Nevada.
- [12] Shah, J., and Mantyla, M., 1995, *Parametric and Feature-based CAD/CAM*, Wiley-inter-science.
- [13] Qian, X., and Dutta, D., 1998, "Features in the Layered Manufacturing of Heterogeneous Objects," *Symposium of Solid Freeform Fabrication*, The University of Texas at Austin, pp. 689–696, Aug.
- [14] Regli, W. C., and Pratt, M. J., 1996, "What are Feature Interactions," *Proceedings of The 1996 ASME Design Engineering Technical Conference and Computers in Engineering Conference*, Aug, 18–22, Irvine, Ca.
- [15] Qian, X., and Dutta, D., 1999, "Feature-based Fabrication in Layered Manufacturing," Technical Report UM-MEAM-99-13, the University of Michigan, Nov.
- [16] NIST Design, Processing Planning and Assembly Repository, <http://www.mel.nist.gov/ppth/>